Correlation Matrix Techniques at Non-Zero Momentum

Benjamin J. Menadue[a,*], Waseem Kamleh[a], Derek B. Leinweber[a], M. Selim Mahbub[a], Benjamin J. Owen[a]

[a] *Special Research Centre for the Subatomic Structure of Matter, School of Chemistry & Physics, University of Adelaide, South Australia 5005, Australia*

arXiv:1302.4152v1 [hep-lat] 18 Feb 2013

Abstract

In recent years, the use of variational analysis techniques in lattice QCD has been demonstrated to be remarkably successful in the investigation of the rest-mass spectrum of many hadrons. However, due to parity-mixing, more care must be taken for investigations of boosted states to ensure that the projected correlation functions provided by the variational analysis correspond to the same states at zero momentum. In this Letter we demonstrate a novel method for ensuring the successful and consistent isolation of boosted states by expanding the operator basis used to construct the correlation matrix to include operators of the opposite parity.

Keywords: baryon, excited state, variational analysis, non-zero momentum, lattice QCD

1. Introduction

One of the greatest successes of lattice QCD has been its application to hadron spectroscopy. The rest masses of not only the ground states, but also many excited states, can be extracted with relative ease through a combination of effective mass techniques and variational analysis. For example, there has been significant recent success by the CSSM Lattice Collaboration [1–4], the BGR Collaboration [5], and the HSC Collaboration [6].

Once an understanding of the spectra is obtained, the logical progression is to investigate the structure of these hadrons, and again lattice QCD has provided the tools needed for precise determination of quantities such as the Sachs form factors, charge radii, and magnetic moments. To date, however, such analyses have primarily focussed on the ground states and the current-induced parity transitions.

Key to lattice QCD's ability to investigate hadronic structure is the computation of two- and three-point correlation functions for each hadronic state of interest at both zero and non-zero final state momenta. While the zero momentum two-point case corresponds the rest mass analysis and is well understood, at non-zero momentum more care must be taken with baryons to ensure the correct correlation functions are extracted, especially when investigating excited states.

In this Letter, we investigate the use of variational analysis techniques to extract correlation functions for excited states of baryons at non-zero momentum. In Sections 2 and 3 we describe the traditional approaches and highlight how states of the opposite parity can intrude into the analysis. Section 4 demonstrates a novel method for overcoming this shortfall. This method will be central to future baryon form-factor calculations involving excited states, for example, electromagnetic structure and transition analyses.

The results presented in Section 4 are calculated on the PACS-CS (2 + 1)-flavour full-QCD ensembles [7], made available through the ILDG [8]. They are $32^3 \times 64$ lattices with $\beta = 1.90$, and employ an Iwasaki gauge action with non-perturbatively $O(a)$-improved Wilson quarks. In particular, we demonstrate proof of principle on the ensemble with the heaviest quark mass, with $\kappa_{\mathrm{u,d}} = 0.137$, corresponding to a pion mass of 702 MeV.

2. Ground State Analysis

To extract the mass for the ground state of a baryon, consider an interpolating operator[1] χ that couples to this baryon and construct the corresponding two-point correlation function,

$$\mathcal{G}(\mathbf{p}; t) = \sum_{\mathbf{x}} \mathrm{e}^{-\mathrm{i}\,\mathbf{p}\cdot\mathbf{x}} \langle \Omega | \chi(x) \overline{\chi}(0) | \Omega \rangle \,. \tag{1}$$

By inserting a complete set of states $\mathbb{I} = \sum |B; p; s\rangle \langle B; p; s|$ between operators and noting our use of Euclidean time, we can rewrite this as

$$\mathcal{G}(\mathbf{p}; t) = \sum_{B} \sum_{s} \mathrm{e}^{-E_B(\mathbf{p})\, t} \langle \Omega | \chi(0) | B; p; s \rangle \langle B; p; s | \overline{\chi}(0) | \Omega \rangle \,, \tag{2}$$

where $E_B(\mathbf{p}) = (m_B^2 + |\mathbf{p}|^2)^{1/2}$ is the energy of state $|B\rangle$ at momentum $\mathbf{p}$, and m_B is its mass.

Let us now define coupling constants λ_B and $\overline{\lambda}_B$ such that

$$\begin{aligned} \langle \Omega | \chi | B^+; p; s \rangle &= \lambda_{B^+} \sqrt{\frac{m_{B^+}}{E_{B^+}}}\, u_{B^+}(p, s) \text{ and} \\ \langle B^+; p; s | \overline{\chi} | \Omega \rangle &= \overline{\lambda}_{B^+} \sqrt{\frac{m_{B^+}}{E_{B^+}}}\, \overline{u}_{B^+}(p, s) \end{aligned} \tag{3}$$

[1] In general these operators are not definite in parity, so that while they may transform as positive- or negative-parity operators, they couple to both positive- and negative-parity states.

*Corresponding author.

for positive-parity states $|B^+\rangle$, and

$$\langle\Omega|\chi|B^-;p;s\rangle = \lambda_{B^-}\sqrt{\frac{m_{B^-}}{E_{B^-}}}\,\gamma_5\,u_{B^-}(p,s) \text{ and}$$
$$\langle B^-;p;s|\overline{\chi}|\Omega\rangle = -\overline{\lambda}_{B^-}\sqrt{\frac{m_{B^-}}{E_{B^-}}}\,\overline{u}_{B^-}(p,s)\,\gamma_5 \tag{4}$$

for negative-parity states $|B^-\rangle$, where $u_{B^\pm}$ and $\overline{u}_{B^\pm}$ are positive-parity Dirac spinors. This substitution allows us to write the spin sum as

$$\sum_s u_{B^\pm}(p,s)\,\overline{u}_{B^\pm}(p,s) = \frac{\gamma\cdot p + m_{B^\pm}}{2m_{B^\pm}}, \tag{5}$$

and we can split Equation (2) into positive- and negative-parity components:

$$\mathcal{G}(\mathbf{p};t) = \sum_{B^+}\lambda_{B^+}\,\overline{\lambda}_{B^+}\,\mathrm{e}^{-E_{B^+}t}\frac{\gamma\cdot p + m_{B^+}}{2E_{B^+}} + \sum_{B^-}\lambda_{B^-}\,\overline{\lambda}_{B^-}\,\mathrm{e}^{-E_{B^-}t}\frac{\gamma\cdot p - m_{B^-}}{2E_{B^-}}. \tag{6}$$

At this point, we construct a new correlation function by taking the spinor trace of $\mathcal{G}$ with some Dirac matrix Γ:

$$G(\Gamma;\mathbf{p};t) = \mathrm{tr}(\Gamma\,\mathcal{G}(\mathbf{p};t)). \tag{7}$$

In particular, by taking $\Gamma = \Gamma^+ := (\gamma^0 + \mathbb{I})/2$ we get

$$G(\Gamma^+;\mathbf{p};t) = \sum_{B^+}\lambda_{B^+}\,\overline{\lambda}_{B^+}\,\mathrm{e}^{-E_{B^+}t}\frac{E_{B^+} + m_{B^+}}{E_{B^+}} + \sum_{B^-}\lambda_{B^-}\,\overline{\lambda}_{B^-}\,\mathrm{e}^{-E_{B^-}t}\frac{E_{B^-} - m_{B^-}}{E_{B^-}}, \tag{8}$$

and by taking $\Gamma = \Gamma^- := (\gamma^0 - \mathbb{I})/2$,

$$G(\Gamma^-;\mathbf{p};t) = \sum_{B^+}\lambda_{B^+}\,\overline{\lambda}_{B^+}\,\mathrm{e}^{-E_{B^+}t}\frac{E_{B^+} - m_{B^+}}{E_{B^+}} + \sum_{B^-}\lambda_{B^-}\,\overline{\lambda}_{B^-}\,\mathrm{e}^{-E_{B^-}t}\frac{E_{B^-} + m_{B^-}}{E_{B^-}}. \tag{9}$$

At zero momentum, $m_B = E_B$, and so $\Gamma^\pm$ act as parity projectors, allowing us to separate out and individually examine the positive- and negative-parity contributions. Furthermore, in the limit as $t \to \infty$, only the lowest lying state will remain, so that

$$G(\Gamma^\pm;\mathbf{0};t) \overset{\text{large } t}{\sim} 2\lambda_{B_0^\pm}\,\overline{\lambda}_{B_0^\pm}\,\mathrm{e}^{-m_{B_0^\pm}t}, \tag{10}$$

where $|B_0^\pm\rangle$ are the lowest-lying, positive- and negative-parity states. This allows us to easily extract the masses of the positive- and negative-parity ground states by defining the positive- and negative-parity effective masses of a correlation function G as

$$M_{\text{eff}}^\pm(t) := \ln\frac{G(\Gamma^\pm;\mathbf{0};t)}{G(\Gamma^\pm;\mathbf{0};t+1)} \overset{\text{large } t}{\sim} m_{B_0^\pm}. \tag{11}$$

At non-zero momentum, $m_B \neq E_B$, and so $\Gamma^\pm$ do not act as perfect parity projectors; contaminations from states of the opposite parity are introduced because the boost to non-zero momentum begins to mix the parities. This situation was investigated in [9], where a projector of the form

$$\Gamma^\pm(\mathbf{p}) := \frac{1}{2}\left(\frac{m_{B_0^\mp}}{E_{B_0^\mp}(\mathbf{p})}\gamma_0 \pm \mathbb{I}\right), \tag{12}$$

was introduced to remove a single contaminating state, the lowest state of the opposite parity. If this is the only nearby contaminating state, this projector allows for the definition of an effective energy in the same fashion as the effective mass in Equation (11):

$$E_{\text{eff}}^\pm(\mathbf{p},t) := \ln\frac{G(\Gamma^\pm(\mathbf{p});\mathbf{p};t)}{G(\Gamma^\pm(\mathbf{p});\mathbf{p};t+1)} \overset{\text{large } t}{\sim} E_{B_0^\pm}(\mathbf{p}). \tag{13}$$

However, if there is more than one nearby state contaminating the correlation function, this large-t approximation will again fail.

3. Excited State Analysis

The situation is potentially more challenging when using variational techniques. Here, we consider not just an individual interpolating operator χ in isolation, as in Equation (1), but the $n \times n$ correlation matrix $\mathcal{G}(\mathbf{p};t)$ formed from the cross-correlation functions between n different operators χ_i, $i = 1,\ldots,n$ [1–4, 10, 11]. That is,

$$\mathcal{G}_{ij}(\mathbf{p};t) := \sum_{\mathbf{x}}\mathrm{e}^{-\mathrm{i}\,\mathbf{p}\cdot\mathbf{x}}\,\langle\Omega|\chi_i(x)\overline{\chi}_j(0)|\Omega\rangle\,. \tag{14}$$

As before, we can parameterise the correlation matrix in terms of coupling constants λ_i^α and $\overline{\lambda}_i^\alpha$, this time of each operator (i) to each state (α), to obtain

$$\mathcal{G}_{ij}(\mathbf{p};t) = \sum_{B^+}\lambda_i^{B^+}\,\overline{\lambda}_j^{B^+}\,\mathrm{e}^{-E_{B^+}t}\frac{\gamma\cdot p + m_{B^+}}{2E_{B^+}} + \sum_{B^-}\lambda_i^{B^-}\,\overline{\lambda}_j^{B^-}\,\mathrm{e}^{-E_{B^-}t}\frac{\gamma\cdot p - m_{B^-}}{2E_{B^-}}, \tag{15}$$

and we can again take the spinor trace with an arbitrary Dirac matrix Γ to get

$$G_{ij}(\Gamma;\mathbf{p};t) := \mathrm{tr}(\Gamma\,\mathcal{G}_{ij}(\mathbf{p};t)) = \sum_B\lambda_i^B\,\overline{\lambda}_j^B\,\mathrm{e}^{-E_B t}\,C(\Gamma;B;p), \tag{16}$$

where

$$C(\Gamma;B^\pm;p) := \mathrm{tr}\left(\Gamma\,\frac{\gamma\cdot p \pm m_{B^\pm}}{2E_{B^\pm}(\mathbf{p})}\right) \tag{17}$$

encapsulates the kinematics of the state $B^\pm$.

We define a set of "perfect" operators $\{\,\phi^\alpha\,\}$ that perfectly isolate individual energy eigenstates, so that

$$\langle\Omega|\phi^\alpha|B^\beta;p;s\rangle = \delta^{\alpha\beta}\sqrt{\frac{m_{B^\alpha}}{E_{B^\alpha}}}\,z^\alpha\,u^\alpha(p,s) \text{ and}$$
$$\langle B^\beta;p;s|\phi^\alpha|\Omega\rangle = \delta^{\alpha\beta}\sqrt{\frac{m_{B^\alpha}}{E_{B^\alpha}}}\,\overline{z}^\alpha\,\overline{u}^\alpha(p,s). \tag{18}$$

Using the linearity of the operator space, these can be written as linear combinations of the original operators[2], with

$$\overline{\phi}^{\alpha} = \sum_{i=1}^{n} u_i^{\alpha}\,\overline{\chi}_i \quad \text{and} \quad \phi^{\alpha} = \sum_{i=1}^{n} v_i^{\alpha}\,\chi_i. \tag{19}$$

Then, acting on Equation (16) from the right with the coefficient vector $\mathbf{u}^{\alpha} := (u_1^{\alpha}, \ldots, u_n^{\alpha})$ and similarly from the left with $\mathbf{v}^{\alpha} := (v_1^{\alpha}, \ldots, v_n^{\alpha})$, we obtain

$$\begin{aligned} G(\Gamma;\mathbf{p};t)\,\mathbf{u}^{\alpha} &= \lambda^{\alpha}\,\overline{z}^{\alpha}\,\mathrm{e}^{-E_{\alpha}\,t}\,C(\Gamma;\alpha;p) \text{ and} \\ \mathbf{v}^{\alpha\top}\,G(\Gamma;\mathbf{p};t) &= z^{\alpha}\,\overline{\lambda}^{\alpha}\,\mathrm{e}^{-E_{\alpha}\,t}\,C(\Gamma;\alpha;p), \end{aligned} \tag{20}$$

where $\lambda^{\alpha} := (\lambda_i^{\alpha}, \ldots, \lambda_n^{\alpha})$, and similarly for $\overline{\lambda}^{\alpha}$. Moreover, acting on $G(\Gamma;\mathbf{p};t)$ with both $\mathbf{u}^{\alpha}$ and $\mathbf{v}^{\alpha}$ at the same time produce a diagonal, fully eigenstate-projected correlation matrix, $\mathbf{v}^{\alpha\top}\,G(\Gamma;\mathbf{p};t)\,\mathbf{u}^{\beta} = \delta^{\alpha\beta}\,z^{\alpha}\,\overline{z}^{\beta}\,\mathrm{e}^{-E_{\alpha}\,t}\,C(\Gamma;\alpha;p)$, and hence we can construct correlation functions that contain single energy eigenstates by

$$G^{\alpha}(\Gamma;\mathbf{p};t) := \mathbf{v}^{\alpha\top}\,G(\Gamma;\mathbf{p};t)\,\mathbf{u}^{\alpha} = z^{\alpha}\,\overline{z}^{\alpha}\,\mathrm{e}^{-E_{\alpha}\,t}\,C(\Gamma;\alpha;p). \tag{21}$$

With the t dependence in Equation (20) constrained to the exponents, it is natural to write recurrence relations in t such that

$$\begin{aligned} G(\Gamma;\mathbf{p};t+\Delta t)\,\mathbf{u}^{\alpha} &= \mathrm{e}^{-E_{\alpha}\,\Delta t}\,G(\Gamma;\mathbf{p};t)\,\mathbf{u}^{\alpha} \text{ and} \\ \mathbf{v}^{\alpha\top}\,G(\Gamma;\mathbf{p};t+\Delta t) &= \mathrm{e}^{-E_{\alpha}\,\Delta t}\,\mathbf{v}^{\alpha\top}\,G(\Gamma;\mathbf{p};t). \end{aligned} \tag{22}$$

That is, the coefficient vectors $\mathbf{u}^{\alpha}$ and $\mathbf{v}^{\alpha}$ are the right and left generalised eigenvectors of $G(\Gamma;\mathbf{p};t+\Delta t)$ and $G(\Gamma;\mathbf{p};t)$, with generalised eigenvalue $\mathrm{e}^{-E_{\alpha}\,\Delta t}$.

Importantly, for sufficiently large n, the lowest-lying states will preferentially be isolated, with all higher excited state contaminations constrained to the highest few states extracted. In extending an analysis from considering just the ground state, as in Section 2, the naïve approach is to continue to use the same Dirac matrix Γ in the parity projection, under the expectation that all states isolated would be of a single parity. Indeed, at zero momentum this is the case, since the parity projection is perfect.

At non-zero momentum, however, the states of the opposite parity again contribute to the parity-projected correlation matrix, and it is therefore possible the correlation matrix analysis will isolate these contaminating states instead. The modified projectors of Equation (12) can remove only a single state of the wrong parity, leaving any other low-lying states of that parity alone to continue contaminating the analysis. Consequently, another approach is needed to ensure the reliability of variational analysis techniques in extracting individual energy eigenstates.

[2]This assumes that the set $\{\chi_i\}$ of original operators spans the operator space. In reality, we are unlikely to have enough operators to completely span the space. In this case, the equality becomes an approximation, albeit improving as the number n of operators used increases. The approximation can also be improved by performing the analysis at later times t and $t+\Delta t$ in Equation (22) since the Euclidean time evolution suppresses excited state contributions.

4. Using an Expanded Operator Basis

Instead of attempting to remove the contaminating states of the opposite parity, such as through the modified projectors, and analysing the positive- or negative-parity channels individually, we analyse both channels simultaneously using a single, expanded correlation matrix. This expanded matrix is formed by recognising that if χ_i is an interpolating operator that couples to the sector of interest, then so is $\gamma_5\chi_i$ (except it transforms with the opposite parity). Moreover, the sets $\{\chi_i\}$ and $\{\gamma_5\chi_i\}$ are pairwise linearly independent (indeed, at zero momentum the subspaces spanned by each set are disjoint). Correspondingly, the adjoint sets are $\{\overline{\chi}_i\}$ and $\{-\overline{\chi}_i\,\gamma_5\}$.

If the $\mathcal{G}_{ij}(\mathbf{p};t)$ of equation (14) corresponds to the correlation function formed from operators χ_i and $\overline{\chi}_j$, then the corresponding correlation function for $\gamma_5\chi_i$ and $\overline{\chi}_j$ is

$$\begin{aligned} \mathcal{G}_{i'j}(\mathbf{p};t) &= \sum_{\mathbf{x}} \mathrm{e}^{-\mathrm{i}\,\mathbf{p}\cdot\mathbf{x}}\,\langle\Omega|\,\gamma_5\chi_i(x)\overline{\chi}_j(0)|\Omega\rangle \\ &= \sum_{\mathbf{x}} \mathrm{e}^{-\mathrm{i}\,\mathbf{p}\cdot\mathbf{x}}\,\gamma_5\,\langle\Omega|\chi_i(x)\overline{\chi}_j(0)|\Omega\rangle \\ &= \gamma_5\,\mathcal{G}_{ij}(\mathbf{p};t), \end{aligned} \tag{23}$$

where we have introduced a prime on the index to denote the extra γ_5 in the interpolator. Similarly, the correlation functions for χ_i and $-\overline{\chi}_j\,\gamma_5$, and $\gamma_5\chi_i$ and $-\overline{\chi}_j\,\gamma_5$, are $\mathcal{G}_{ij'}(\mathbf{p};t) = -\mathcal{G}_{ij}(\mathbf{p};t)\,\gamma_5$ and $\mathcal{G}_{i'j'}(\mathbf{p};t) = -\gamma_5\,\mathcal{G}_{ij}(\mathbf{p};t)\,\gamma_5$, respectively. Then, using the invariance of the trace operation under cyclic permutations, for a Dirac matrix Γ the associated "projected" correlation functions are, in the same order,

$$G_{i'j}(\Gamma;\mathbf{p};t) = \mathrm{tr}(\Gamma\,\gamma_5\,\mathcal{G}_{ij}(\mathbf{p};t)) = G_{ij}(\Gamma\,\gamma_5;\mathbf{p};t), \tag{24}$$

$$G_{ij'}(\Gamma;\mathbf{p};t) = -\,\mathrm{tr}(\Gamma\,\mathcal{G}_{ij}(\mathbf{p};t)\gamma_5) = -G_{ij}(\gamma_5\,\Gamma;\mathbf{p};t), \tag{25}$$

and

$$G_{i'j'}(\Gamma;\mathbf{p};t) = -\,\mathrm{tr}(\Gamma\,\gamma_5\,\mathcal{G}_{ij}(\mathbf{p};t)\,\gamma_5) = -G_{ij}(\gamma_5\,\Gamma\,\gamma_5;\mathbf{p};t). \tag{26}$$

Hence, we can write the expanded matrix in block form as

$$G'(\Gamma;\mathbf{p};t) := \begin{bmatrix} G(\Gamma;\mathbf{p};t) & G(\Gamma\,\gamma_5;\mathbf{p};t) \\ G(-\gamma_5\Gamma;\mathbf{p};t) & G(-\gamma_5\,\Gamma\,\gamma_5;\mathbf{p};t) \end{bmatrix} \tag{27}$$

This matrix will not be singular if the original $n\times n$ matrix is also non-singular, and hence we can use it to isolate twice as many states to compensate for the presence of the additional states of opposite parity at non-zero momentum. Since the operators should couple more strongly to states of the same parity as that which they transform as (in the case of $\Gamma^{\pm}$, from Equations (8) and (9) the effective coupling goes as $E+m\sim 2m$ for states of the same parity and $E-m\sim 0$ for the opposite), this expanded correlation matrix is nearly block diagonal. Hence, the eigenvectors corresponding to a state of one parity should be nearly orthogonal to those of states of the opposite parity, as expected.

We can gain insight into the amount of "leakage" between parities by considering the elements of the eigenvectors corresponding to operators of the opposite parity. In Figure 1, we plot

#	**p** (l.u.)	|**p**| (GeV)
1	$(0,0,0)$	0.000
2	$(1,0,0)$	0.427
3	$(1,1,0)$	0.604
4	$(1,1,1)$	0.740
5	$(2,0,0)$	0.854
6	$(2,1,0)$	0.955
7	$(2,1,1)$	1.046
8	$(2,2,0)$	1.208
9	$(3,0,0)$	1.281

Table 1: Momenta used in this analysis.

the eigenvector associated with the positive-parity, ground state Λ as a function of momentum-squared, and in Figure 2, the eigenvector associated with the negative-parity $\Lambda(1405)$. Here, we use the 12×12 expanded correlation matrix formed from the operators χ_1^Λ, χ_2^Λ, and χ^{Λ_S} (Equations (2.5a), (2.5b), and (2.7) of [12]) with 16 and 100 sweeps of gauge-invariant Gaussian smearing [13], where $\Gamma = \Gamma^+ := (\mathbb{I} + \gamma^0)/2$.

We can clearly recognise the effect of Lorentz contraction in increasing the overlap of less smeared operators at large momenta, as demonstrated in [14]. In both Figures 1 and 2, the dominant two same-parity components correspond to the same flavour structure—χ_1^Λ for the Λ and χ^{Λ_S} for the $\Lambda(1405)$—but with different amounts of smearing. At low momentum, the dominant smearing is the 100 sweeps, while as the momentum increases the contribution from the smaller 16 sweep source increases. We suspect the two discontinuities in this trend, between the fourth and fifth, and eighth and ninth momenta, are due to the lack of SO(3) rotational invariance on the lattice; they correspond to the transitions from momenta diagonal across the lattice to momenta purely in the x-direction. The momenta used are tabulated in Table 1.

5. Conclusion

While the relative sizes of the eigenvector components associated with opposite-parity operators are small ($\lesssim$ 5%) compared to the dominant same-parity component, they are nonetheless non-zero and, if neglected by only using the traditional non-extended correlation matrix, prohibit the clean isolation of energy eigenstates. As we have demonstrated in this Letter, by extending the correlation matrix to include operators of the opposite parity, we can investigate and cleanly isolate both parity channels at the same time. Moveover, since the parity transformation amounts to simply pre- or post-multiplying (or both) the projection matrix Γ by γ_5, it is a computationally inexpensive procedure.

Acknowledgements

This research was undertaken with the assistance of resources at the NCI National Facility in Canberra, Australia, and the iVEC facilities at Murdoch University (iVEC@Murdoch) and the University of Western Australia (iVEC@UWA). These resources were provided through the National Computational Merit Allocation Scheme, supported by the Australian Government. This research is supported by the Australian Research Council.

References

References

[1] M. S. Mahbub, A. Ó. Cais, W. Kamleh, B. G. Lasscock, D. B. Leinweber, A. G. Williams, Isolating Excited States of the Nucleon in Lattice QCD, Phys. Rev. D 80 (2009) 054507. `arXiv:0905.3616`, `doi:10.1103/PhysRevD.80.054507`.

[2] M. S. Mahbub, W. Kamleh, D. B. Leinweber, P. J. Moran, A. G. Williams, Roper Resonance in 2+1 Flavor QCD, Phys. Lett. B 707 (2012) 389. `arXiv:1011.5724`, `doi:10.1016/j.physletb.2011.12.048`.

[3] B. J. Menadue, W. Kamleh, D. B. Leinweber, M. Mahbub, Extracting Low-Lying Lambda Resonances Using Correlation Matrix Techniques, AIP Conf. Proc. 1354 (2011) 213. `arXiv:1102.3492`, `doi:10.1063/1.3587609`.

[4] B. J. Menadue, W. Kamleh, D. B. Leinweber, M. S. Mahbub, Isolating the $\Lambda(1405)$ in Lattice QCD, Phys. Rev. Lett. 108 (2012) 112001. `arXiv:1109.6716`, `doi:10.1103/PhysRevLett.108.112001`.

[5] G. P. Engel, C. Lang, A. Schäfer, Low-lying Λ Baryons from the Lattice`arXiv:1212.2032`.

[6] J. Bulava, R. Edwards, E. Engelson, B. Joó, H.-W. Lin, et al., Nucleon, Δ and Ω excited states in $N_f = 2+1$ lattice QCD, Phys. Rev. D 82 (2010) 014507. `arXiv:1004.5072`, `doi:10.1103/PhysRevD.82.014507`.

[7] S. Aoki, K.-I. Ishikawa, N. Ishizuka, T. Izubuchi, D. Kadoh, K. Kanaya, Y. Kuramashi, Y. Namekawa, M. Okawa, Y. Taniguchi, A. Ukawa, N. Ukita, T. Yoshie, 2+1 Flavor Lattice QCD toward the Physical Point, Phys. Rev. D 79 (2009) 034503. `arXiv:0807.1661`, `doi:10.1103/PhysRevD.79.034503`.

[8] M. G. Beckett, P. Coddington, B. Joó, C. M. Maynard, D. Pleiter, O. Tatebe, T. Yoshie, Building the International Lattice Data Grid, Comput. Phys. Commun. 182 (2011) 1208. `arXiv:0910.1692`, `doi:10.1016/j.cpc.2011.01.027`.

[9] F. X. Lee, D. B. Leinweber, Negative parity baryon spectroscopy, Nucl. Phys. Proc. Suppl. 73 (1999) 258. `arXiv:hep-lat/9809095`, `doi:10.1016/S0920-5632(99)85041-5`.

[10] C. Michael, Adjoint Sources in Lattice Gauge Theory, Nucl. Phys. B 259 (1985) 58. `doi:10.1016/0550-3213(85)90297-4`.

[11] M. Lüscher, U. Wolff, How To Calculate The Elastic Scattering Matrix In Two-Dimensional Quantum Field Theories By Numerical Simulation, Nucl. Phys. B 339 (1990) 222. `doi:10.1016/0550-3213(90)90540-T`.

[12] D. B. Leinweber, R. Woloshyn, T. Draper, Electromagnetic structure of octet baryons, Phys. Rev. D 43 (1991) 1659. `doi:10.1103/PhysRevD.43.1659`.

[13] S. Güsken, A Study of smearing techniques for hadron correlation functions, Nucl. Phys. Proc. Suppl. 17 (1990) 361. `doi:10.1016/0920-5632(90)90273-W`.

[14] D. S. Roberts, W. Kamleh, D. B. Leinweber, M. Mahbub, B. J. Menadue, Accessing High Momentum States In Lattice QCD, Phys. Rev. D 86 (2012) 074504. `arXiv:1206.5891`, `doi:10.1103/PhysRevD.86.074504`.

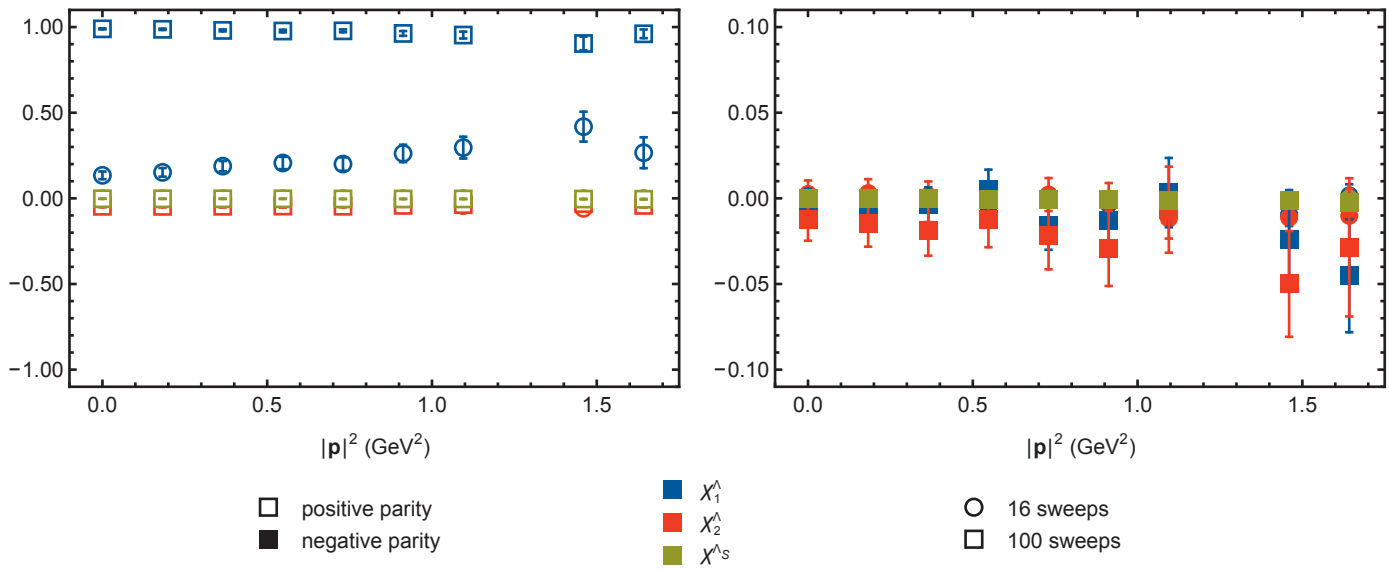

Figure 1: (colour online) Momentum-squared dependence of the eigenvector associated with the positive-parity, ground state Λ. Components associated with operators of the same parity are indicated in the left plot while components associated with operators of the opposite parity are illustrated in the right plot. At zero momentum, all opposite-parity components are consistent with zero within errors. Eigenvectors are normalised so that they have unit 2-norm and positive maximal–absolute-value component.

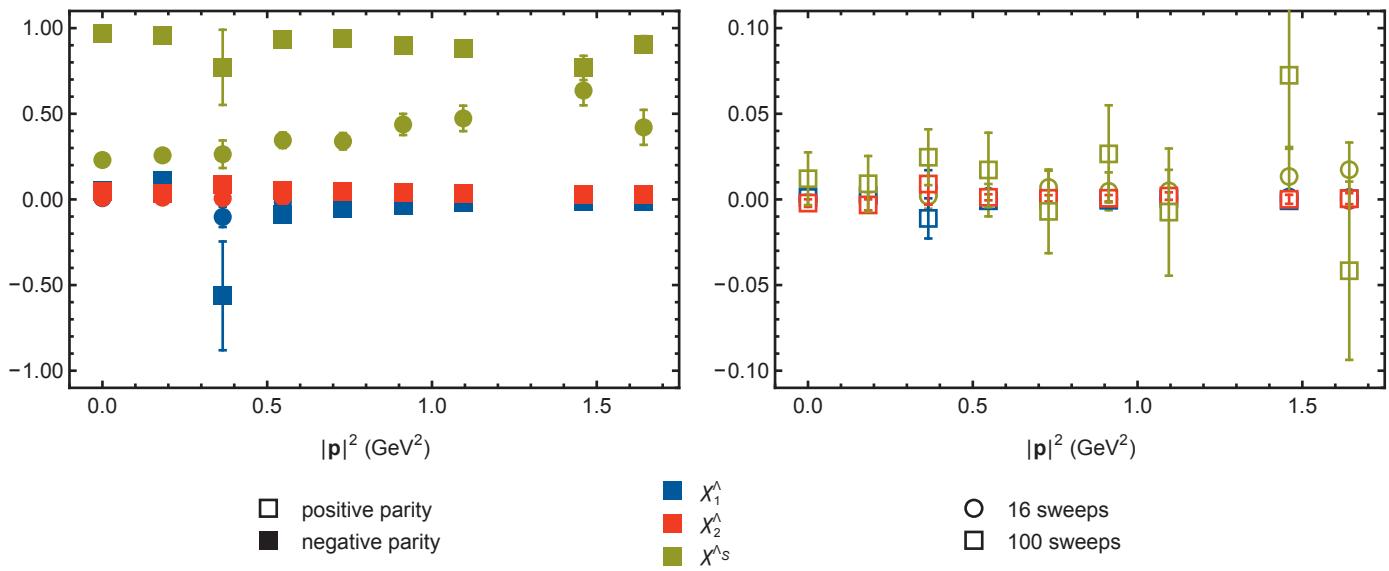

Figure 2: (colour online) Momentum-squared dependence of the eigenvector associated with the negative-parity $\Lambda(1405)$. Components associated with operators of the same parity are indicated in the left plot while components associated with operators of the opposite parity are illustrated in the right plot. At zero momentum, all opposite-parity components are consistent with zero within errors. Eigenvectors are normalised so that they have unit 2-norm and positive maximal–absolute-value component.